A Triangle−Square Equilibrium of Metallosupramolecular Assemblies Based on Pd(II) and Pt(II) Corners and Diazadibenzoperylene Bridging Ligands

Armin Sautter,[†] Dietmar G. Schmid,[‡] Günther Jung,[‡] and Frank Würthner*,[†]

Contribution from the Department of Organic Chemistry II, University of Ulm, Albert-Einstein-Allee 11, D-89081 Ulm, and the Department of Organic Chemistry, University of Tübingen, Auf der Morgenstelle 18, D-72076 Tübingen, Germany

Received December 27, 2000. Revised Manuscript Received March 15, 2001

Abstract: Tetraaryloxy-substituted diazadibenzoperylene bridging ligands **1a,b** were employed in transition metal-directed self-assembly with Pd(II) and Pt(II) phosphane triflates **2a,b** which resulted in complex dynamic equilibria between molecular triangles **3a**−**d** and molecular squares **4a**−**d** in solution. Characterization of the equilibria and assignment of the metallacycles was accomplished by ^{1}H and ^{31}P{^{1}H} NMR spectroscopy in combination with electrospray ionization Fourier transform ion cyclotron mass spectrometry (ESI-FTICR-MS). It was found that the equilibria depend on several factors, such as the metal ion (Pd^{2+} or Pt^{2+}), the solvent, and the steric demand of the phenoxy substituents of the diazadibenzoperylene ligands **1a,b**. Introduction of bulky *tert*-butyl groups in **1b** shifts the equilibrium significantly in the direction of the molecular squares. Molecular dynamics simulations of the triangle and square structures revealed critical steric effects and restricted conformational flexibilities of the phosphane and diazadibenzoperylene ligands that help explain the distinct dynamic behavior observed in variable-temperature NMR studies. Concentration-dependent UV/vis and fluorescence spectroscopy revealed the limited stability of the assemblies and confirmed the reversible nature of the dynamic equilibria.

Introduction

Transition metal-directed self-assembly of macrocycles and cage compounds has received considerable attention lately, leading to more and more complex architectures,[1] for example, molecular triangles,[1b,2,3] squares and rectangles,[3,4,5] pentagons and hexagons,[6] catenanes, nanotubes and polytubes,[7] bowls and cages,[8] cuboctahedra and dodecahedra[9] among many others. The possibility to use a wide variety of transition metal ions diversifies this field considerably. The focus of current research is on the introduction of functionality into these systems such as redoxactivity,[4,5] magnetic[4j] or luminescence properties,[4,5,10] and applications such as anion recognition[4d,7b] and electrochemical sensing.[4k] Recently, the incorporation of functional dye ligands, based on perylene bisimides and porphyrins, into metallacycles opened up a promising avenue toward artificial light-harvesting systems.[4f−g,10]

* To whom correspondence should be addressed.
[†] Department of Organic Chemistry II, University of Ulm.
[‡] Department of Organic Chemistry, University of Tübingen.

(1) (a) Lehn, J.-M. *Supramolecular Chemistry*, VCH: Weinheim, 1995. (b) Leininger, S.; Olenyuk, B.; Stang, P. J. *Chem. Rev.* **2000**, *100*, 853−908 and references therein.

(2) (a) Hall, J.; Loeb, S. J.; Shimizu, G. K. H.; Yap, G. P. A. *Angew. Chem., Int. Ed.* **1998**, *37*, 121−123. (b) Thompson, A.; Rettig, S. J.; Dolphin, D. *Chem. Commun.* **1999**, 631−632. (c) Habereder, T.; Warchhold, M.; Nöth, H.; Severin, K. *Angew. Chem., Int. Ed.* **1999**, *38*, 3225−3228. (d) Lai, S.-W.; Chan, M. C.-W.; Peng, S.-M.; Che, C.-M. *Angew. Chem., Int. Ed.* **1999**, *38*, 669−671. (e) Schnebeck, R.-D.; Freisinger, E.; Glahe, F.; Lippert, B. *J. Am. Chem. Soc.* **2000**, *122*, 1381−1390. (f) Schnebeck, R.-D.; Randaccio, L.; Zangrando, E.; Lippert, B. *Angew. Chem., Int. Ed.* **1998**, *37*, 119−121. (g) Schnebeck, R.-D.; Freisinger, E.; Lippert, B. *Chem. Commun.* **1999**, 675−676. (h) Barbera, J.; Elduque, A.; Gimenez, R.; Oro, L. A.; Serrano, J. L. *Angew. Chem., Int. Ed. Engl.* **1996**, *35*, 2832−2835.

(3) (a) Fujita, M.; Ogura, K. *Bull. Chem. Soc. Jpn.* **1996**, *69*, 1471−1482. (b) Fujita, M.; Ogura, K. *Coord. Chem. Rev.* **1996**, *148*, 249−264. (c) Lee, S. B.; Hwang, S.; Chung, D. S.; Yun, H.; Hong, J.-I. *Tetrahedron Lett.* **1998**, *39*, 873−876. (d) Sun, S.-S.; Lees, A. J. *Inorg. Chem.* **1999**, *38*, 4181−4182. (e) Sun, S.-S.; Lees, A. J. *J. Am. Chem. Soc.* **2000**, *122*, 8956−8967. (f) Schnebeck, R.-D.; Freisinger, E.; Lippert, B. *Eur. J. Inorg. Chem.* **2000**, 1193−1200. (g) McQuillan, F. S.; Berridge, T. E.; Chen, H.; Hamor, T. A.; Jones, C. J. *Inorg. Chem.* **1998**, *37*, 4959−4970.

(4) (a) Fujita, M.; Yazaki, J.; Ogura, K. *J. Am. Chem. Soc.* **1990**, *112*, 5645−5647. (b) Stang, P. J.; Cao, D. H. *J. Am. Chem. Soc.* **1994**, *116*, 4981−4982. (c) Stang, P. J.; Olenyuk, B. *Acc. Chem. Res.* **1997**, *30*, 502−518. (d) Slone, R. V.; Yoon, D. I.; Calhoun, R. M.; Hupp, J. T. *J. Am. Chem. Soc.* **1995**, *117*, 11813−11814. (e) Slone, R. V.; Hupp, J. T.; Stern, C.; Albrecht-Schmitt; T. E. *Inorg. Chem.* **1996**, *35*, 4096−4097. (f) Würthner, F.; Sautter, A. *Chem. Commun.* **2000**, 445−446. (g) Würthner, F.; Sautter, A.; Schmid, D. G.; Weber, P. J. A. *Chem. Eur. J.* **2001**, *7*, 894−902. (h) Woessner, S. M.; Helms, J. B.; Houlis, J. F.; Sullivan, B. P. *Inorg. Chem.* **1999**, *38*, 4380−4381. (i) Sun, S.-S.; Silva, A. S.; Brinn, I. M.; Lees, A. J. *Inorg. Chem.* **2000**, *39*, 1344−1345. (j) Campos-Fernandez, C. S.; Clerac, R.; Dunbar, K. R. *Angew. Chem., Int. Ed.* **1999**, *38*, 3477−3479. (k) Lahav, M.; Gabai, R.; Shipway, A. N.; Willner, I. *Chem. Commun.* **1999**, 1937−1938.

(5) (a) Benkstein, K. D.; Hupp, J. T.; Stern, C. L. *J. Am. Chem. Soc.* **1998**, *120*, 12982−12983. (b) Benkstein, K. D.; Hupp, J. T.; Stern, C. L. *Angew. Chem., Int. Ed.* **2000**, *39*, 2891−2893. (c) Benkstein, K. D.; Hupp, J. T.; Stern, C. L. *Inorg. Chem.* **1998**, *37*, 5404−5405. (d) Woessner, S. M.; Helms, J. B.; Shen, Y.; Sullivan, B. P. *Inorg. Chem.* **1998**, *37*, 5406−5407. (e) Hartmann, H.; Berger, S.; Winter, R.; Fiedler, J.; Kaim, W. *Inorg. Chem.* **2000**, *39*, 4977−4980.

(6) (a) Stang, P. J.; Persky, N. E.; Manna, J. *J. Am. Chem. Soc.* **1997**, *119*, 4777−4778. (b) Matsumoto, N.; Motoda, Y.; Matsuo, T.; Nakashima, T.; Re, N.; Dahan, F.; Tuchagues, J.-P. *Inorg. Chem.* **1999**, *38*, 1165−1173. (c) Mamula, O.; von Zelewsky, A.; Bernardinelli, G. *Angew. Chem., Int. Ed.* **1998**, *37*, 289−293. (d) Hasenknopf, B.; Lehn, J.-M.; Baum, G.; Kneisel, B. O.; Fenske, D. *Angew. Chem., Int. Ed. Engl.* **1996**, *35*, 1838−1840.

(7) (a) Fujita, M. *Acc. Chem. Res.* **1999**, *32*, 53−61 and references therein. (b) Aoyagi, M.; Biradha, K.; Fujita, M. *J. Am. Chem. Soc.* **1999**, *121*, 7457−7458. (c) Biradha, K.; Aoyagi, M.; Fujita, M. *J. Am. Chem. Soc.* **2000**, *122*, 2397−2398.

10.1021/ja004360y CCC: $20.00
Published on Web 05/18/2001

There have been many concepts and ideas to predict which species will self-assemble in solution,[1,11] and these considerations are mainly based on the information stored in the building blocks, that is, the number of receptor groups, their positioning in space, the electronic configuration of the metal ions, and the specificity of molecular recognition. It appears from this work that rational design of metallosupramolecular structures is a reliable method. Thus, *cis*-protected square planar Pd(II) corners will assemble to molecular squares in the presence of ditopic linear bridging ligands, whereas angular units of 60° and 120° in combination with linear linkers suffice to form triangles and hexagons, respectively.[2,3,6] However, there is an increasing number of examples that deviate from the expected structures. Often two or more species equilibrate when there is no thermodynamically clearly favored species or when further effects come into play such as steric strain and electrostatic repulsion. Equilibration is facilitated by the reversible nature of the bond-forming−bond-breaking process in the self-assembly of metal−ligand systems that is strongly desired and regarded as a self-repairing option to obtain perfect structures.

The focus of our work is on large-sized molecular triangles and molecular squares, where numerous examples for square structures but considerably less for triangular structures are given in the literature.[2] Besides "pure" squares and triangles, also a few equilibria between molecular squares and triangles have been reported.[3] One of the most useful corner units is given with *cis*-dpppPd(II) and -Pt(II) which were introduced by Stang et al.[4b] To date, these corners are reported to form exclusively molecular squares with linear diazaligands.[12,13] However, during coordination studies of diazadibenzoperylene ligands **1a,b**[14] with these corner units we observed for the first time triangle−square equilibria also for this system. The triangle−square equilibria were characterized by a combination of variable-temperature multinuclear NMR spectroscopy and ESI-FTICR (electrospray ionization Fourier transform ion cyclotron) mass spectrometry. Molecular modeling gave insight into the mutual steric interactions and structural characteristics of both triangles and squares and helped to understand the dynamics observed on the NMR time scale. Furthermore, the optical absorption and fluorescence properties as well as thermodynamic stabilities of the metal complexes were investigated.

Results and Discussion

Preparation of Metallacycles and NMR Studies. Our initial goal was the construction of functional molecular squares and cages via *cis*-protected Pd(II) and Pt(II) phosphane triflates **2a,b** and the new highly fluorescent diazadibenzoperylene ligands **1a,b**.[14] Stoichiometric amounts of **1a** or **1b** and **2a** or **2b** were reacted in dichloromethane at room temperature for 24 h to yield orange complexes in 55−78% isolated yields (Scheme 1).[15] In all cases the bright greenish fluorescence of **1a,b** is quenched immediately upon mixing with **2a,b**, and the solutions turn orange. The isolated crystalline complexes were characterized by elemental analyses (C, H, N, S) that proved the 1:1 stoichiometry for all combinations of diazadibenzoperylene bridging ligands **1a,b** and metal−phosphane corners **2a,b**.[16] On the other hand NMR spectra of these complexes exhibited broad signals in the ^{1}H and two rather broad singlets in the ^{31}P{^{1}H} NMR spectra which did not indicate the formation of the expected molecular squares (Figure 1b).[3,4,13]

The room-temperature NMR spectra implied dynamic processes on the NMR time scale. Therefore, variable-temperature NMR spectra of the **1a**−**2a** complex were recorded in deuterated nitromethane allowing for a wide temperature window (Figure 1). Over the whole temperature range (253−353 K) the ^{31}P-{^{1}H} spectra display two singlets between 10 and 11 ppm that sharpen notably at higher temperatures. The signals are shifted upfield by about 8 ppm with respect to the precursor complex **2a**, typical for aza-ligand coordination.[4f,13] No uncoordinated metal−phosphane corners could be detected. The presence of two ^{31}P resonances indicates two nonequivalent metal−phosphane corner units that are coordinated by **1a**. The ^{1}H NMR spectra show broad and undefined signals at room temperature (Figure 1b), but the signals sharpen at lower temperatures and many defined resonances appear (Figure 1c). However, at higher temperatures, the spectra become simpler, and at 353 K only two sets of signals remain, two for the diazadibenzoperylene ligands **1a** and two for the dppp moiety (Figure 1a). Some signals of the various phenyl groups overlap in the aromatic region, but the α protons next to the coordinating nitrogens at around 9 ppm give well-separated characteristic resonances. In accordance there are two sets of signals present for the propyl bridge of the dppp ligand that overlap themselves but that are well-separated from all other signals. Notably, the integral ratios of corresponding protons of the two sets of signals compare well to those in the ^{31}P{^{1}H} NMR spectrum.

The integral ratio of the ^{31}P{^{1}H} NMR signals was found to be solvent-dependent, changing from 4:6 in deuterated acetonitrile over 5:5 in acetone to about 6:4 in nitromethane. This strongly supports the presence of a thermodynamic equilibrium

(8) (a) Yu, S.-Y.; Kusukawa, T.; Biradha, K.; Fujita, M. *J. Am. Chem. Soc.* **2000**, *122*, 2665−2666. (b) Fujita, M.; Fujita, N.; Ogura, K.; Yamaguchi, K. *Nature* **1999**, *400*, 52−55. (c) Fujita, M.; Yu, S.-Y.; Kusukawa, T.; Funaki, H.; Ogura, K.; Yamaguchi, K. *Angew. Chem., Int. Ed.* **1998**, *37*, 2082−2085.

(9) (a) Takeda, N.; Umemoto, K.; Yamaguchi, K.; Fujita, M. *Nature* **1999**, *398*, 794−796. (b) Olenyuk, B.; Levin, M. D.; Whiteford, J. A.; Shield, J. E.; Stang, P. J. *J. Am. Chem. Soc.* **1999**, *121*, 10434−10435. (c) Olenyuk, B.; Whiteford, J. A.; Fechtenkötter, A.; Stang, P. J. *Nature* **1999**, *398*, 796−799.

(10) (a) Funatsu, K.; Imamura, T.; Ichimura, A.; Sasaki, Y. *Inorg. Chem.* **1998**, *37*, 1798−1804. (b) Drain, C. M.; Lehn, J.-M. *J. Chem. Soc.. Chem. Commun.* **1994**, 2313−2315. (c) Drain, C. M.; Nifiatis, F.; Vasenko, A.; Batteas, J. D. *Angew. Chem., Int. Ed.* **1998**, *37*, 2344−2347. (d) Slone, R. V.; Hupp, J. T. *Inorg. Chem.* **1997**, *36*, 5422−5423. (e) Slone, R. V.; Belanger, S.; Hupp, J. T.; Guzei, I. A.; Rheingold, A. L. *Coord. Chem. Rev.* **1998**, *171*, 221−243. (f) Slone, R. V.; Yoon, D. I.; Calhoun, R. M.; Hupp, J. T. *J. Am. Chem. Soc.* **1995**, *117*, 11813−11814. (g) Iengo, E.; Milani, B.; Zangrando, E.; Geremia, S.; Alessio, E. *Angew. Chem., Int. Ed.* **2000**, *39*, 1096−1099.

(11) (a) Stang, P. J. *Chem. Eur. J.* **1998**, *4*, 19−27. (b) Caulder, D. L.; Raymond, K. N. *Acc. Chem. Res.* **1999**, *32*, 975−982. (c) Navarro, J. A. R.; Lippert, B. *Coord. Chem. Rev.* **1999**, *185*−*186*, 653−667.

(12) Hong et al. (ref 3c) reported a triangle−square equilibrium with enPd$(NO_3)_2$ and *trans*-1,2-bis(4-pyridyl)ethylene. For reasons of characterization by mass spectrometry they prepared the analogous [Pd(dppp)]-[$(OTf)_2$] complex.

(13) Stang, P. J.; Cao, D. H.; Saito, S.; Arif, A. M. *J. Am. Chem. Soc.* **1995**, *117*, 6273−6283. Here, an example is reported with the diaza-ligand pyridazine which did not yield a molecular square but a complex with two pyrazines coordinated to one metal ion. It was reasoned that steric interaction between the phosphane ligands of adjacent metals prevented square formation.

(14) Würthner, F.; Sautter, A.; Thalacker, C. *Angew. Chem., Int. Ed.* **2000**, *39*, 1243−1245.

(15) NMR experiments indicate that the self-assembly process is quantitative because exactly the same ^{1}H and ^{31}P{^{1}H} NMR spectra as for the isolated complexes were observed after mixing stoichiometric amounts of **1** and **2** in $CDCl_3$ in the NMR tube. However, owing to the very good solubility of the complexes in dichloromethane and the formation of extremely fine precipitates upon addition of diethyl ether, the isolated yields are only 55−78%.

(16) All attempts to grow single crystals suitable for X-ray analysis failed. Only very small crystals of poor quality could be obtained which were unstable and immediately cracked upon manipulation or removal from the mother liquor.

Scheme 1. Self-Assembly by Metal−Ligand Coordination of Phenoxy-Substituted Diazadibenzoperylenes **1a,b** and Metal−Phosphane Triflates **2a,b** and Triangle−Square Equilibria **3a−d/4a−d**

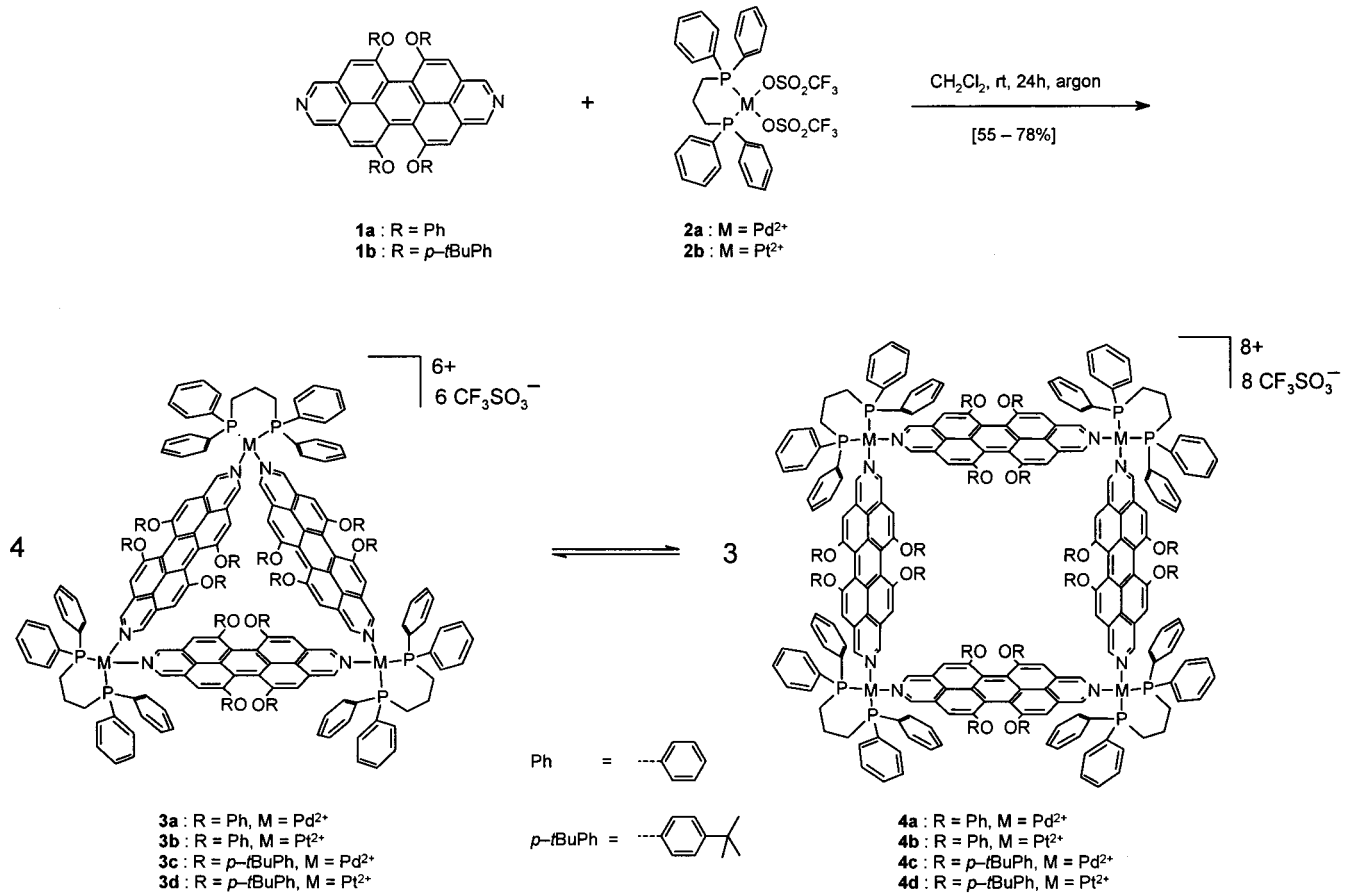

between two different species. Interestingly, dissociation occurs at elevated temperatures ($T > 320$ K) in DMSO as no more sharp signals could be detected but only a broad resonance around $\delta = 20$ ppm.

The NMR spectra of all other complexes between diazaligands **1a,b** and metal corners **2a,b** exhibit the same features as those of complex **1a**−**2a**, that is, temperature dependence and two sets of signals at high temperatures both in the ^{1}H and ^{31}P{^{1}H} NMR spectra, indicating that the same kind of species are formed. However, there are differences in the integral ratios of the two sets of signals for the Pd(II) and the Pt(II) complexes. The ratio in CD_3NO_2 is ca. 2:3 for **1a**−**2a** (Pd(II)) and ca. 1:1 for **1a**−**2b** (Pt(II)). This implies that not one species with two nonequivalent metal−phosphane corner and diazadibenzoperylene ligand units is present, but that two different species must be in equilibrium. This point of view is further supported by complexes that contain the sterically more demanding *tert*-butyl-substituted ligand **1b** which exhibit inverted integral ratios (ca. 7:3 (**1b**−**2a**) and 8:2 (**1b**−**2b**)) with respect to the complexes containing ligand **1a**. Obviously, here the other species is preferred, pointing to a pronounced steric influence of the *tert*-butyl groups on the equilibrium. Figure 2 shows parts of the ^{1}H and ^{31}P{^{1}H} NMR spectra of **1b**−**2b** which exhibit simpler signal patterns (because of the 4-substituted phenoxy groups) and additionally two characteristic singlets for the *tert*-butyl groups in the ^{1}H NMR.[17]

Mass Spectrometry. ESI-FTICR-MS allowed the unambiguous assignment of the species present in the equilibria. This

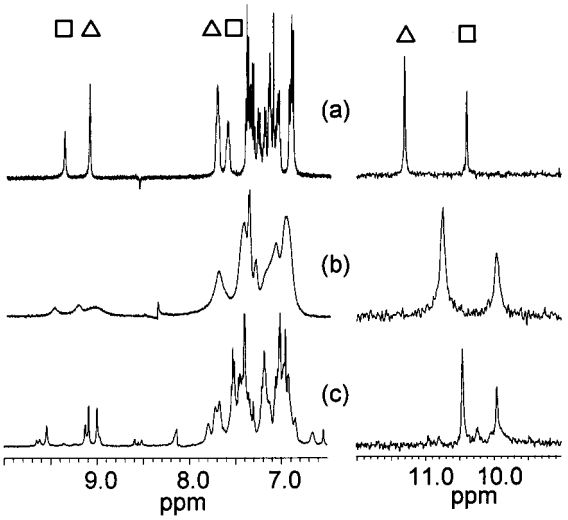

Figure 1. Variable-temperature ^{1}H (left; aromatic part) and ^{31}P{^{1}H} (right) NMR spectra of triangle−square equilibrium **3a/4a** recorded in CD_3NO_2; (a) 353 K; (b) 303 K; (c) 253 K.

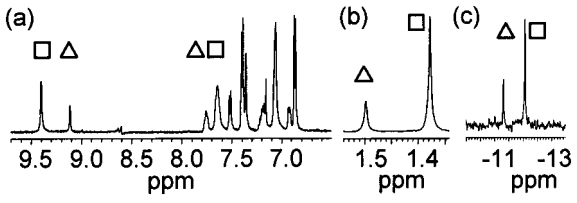

Figure 2. ^{1}H and ^{31}P{^{1}H} NMR spectra of triangle−square equilibrium **3d/4d** recorded in CD_3NO_2 at 353 K; (a) aromatic protons; (b) *tert*-butyl protons; (c) phosphorus nuclei.

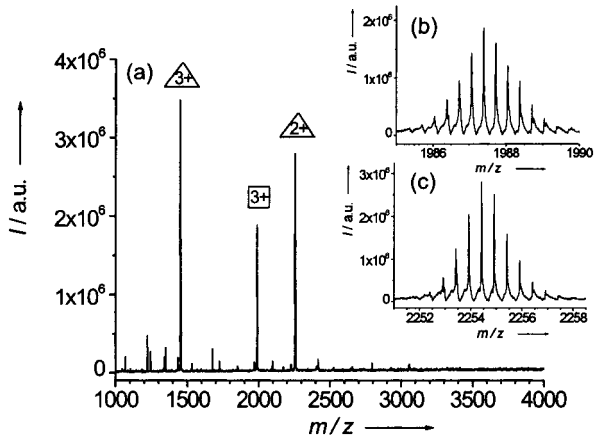

Figure 3. (a) ESI-FTICR-MS (acetone solution) of triangle−square equilibrium **3b/4b**; the insets show the resolved signals of (b) the triply charged square [**4b**-3OTf]$^{3+}$ and (c) the doubly charged triangle [**3b**-2OTf]$^{2+}$.

technique was used because of both its capability of achieving extremely high mass resolution and the possibility of measuring with a very high mass accuracy.[18] With this method signals arising from the isotopic distribution of multiply charged large molecules generated by ESI can be resolved. From the isotopic pattern the charge state can be derived, thus allowing the calculation of the molecular weight. However, only the more stable platinum complexes **1a**−**2b** and **1b**−**2b** could be analyzed. The overview spectrum of system **1a**−**2b** (acetone solution) displays three main signals centered at *m*/*z* 2254.416 with a charge state of $z = 2$, that is, separation of peaks by 0.5 mass units, *m*/*z* 1987.392 ($z = 3$) and *m*/*z* 1453.308 ($z = 3$) (Figure 3). Two signals are magnified to show the isotopic distribution (Figure 3b and c) with a resolution of up to 78 000 (fwhh, full width at half peak height). As the ionization of the complexes occurs simply by the loss of triflate anions, the corresponding deconvolution of the three signals confirms that only two oligomers are present in the equilibrium of a molecular mass of 4807 and 6409. These values correspond exactly to a (**1a**−**2b**)$_3$ trimer (**3b**) and a (**1a**−**2b**)$_4$ tetramer (**4b**). Evidence for the cyclic nature of the species has been provided by the NMR studies allowing us to assign the two species to be the molecular triangle **3b** and the molecular square **4b**.

In contrast to the signals for the trimeric and tetrameric species at *m*/*z* 2254 and *m*/*z* 1987, the signal of the triply charged triangle [**3b**-3OTf]$^{3+}$ at *m*/*z* 1453 is superimposed by a singly charged species with the same *m*/*z* ratio, that is, one perylene ligand and one platinum phosphane corner (Figure 4). This signal (*m*/*z* 1453) serves as a good example to address the general difficulty of unambiguous characterization of large supramolecular structures of high symmetry by mass spectrometry. It could in principle originate from several species different in their charge state *z*, (i) a singly charged fragment consisting of a platinum corner coordinated by one diaza-ligand, (ii) a doubly charged species of two corners and two diaza-ligands ("half-square"), (iii) a triply charged triangular species, (iv) a 4-fold charged square species or (v) higher *n*-fold charged (**1a**−**2b**)$_n$ species. All of these species render the same *m*/*z* ratio but can be distinguished by their charge state and isotopic distributions. Therefore, only the high resolution of the ESI-FTICR method allows the unambiguous determination of the charge states for highly charged species and therefore identification and assignment of the actual species. Figure 4 shows the overlaying of a singly charged species (spacing of the mass peaks by one mass unit) and a triply charged species (spacing of 1/3) corresponding to (i) and (iii), and the signal pattern matches well with the overlaying of the corresponding calculated spectra.

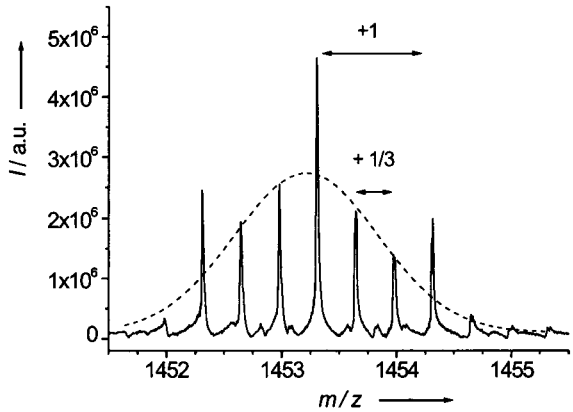

Figure 4. Superposition of signals arising from the triply charged triangle [**3b**-3OTf]$^{3+}$ and a simply charged fragment (one perylene ligand and one platinum phosphane corner). Both species exhibit the same *m*/*z* ratio, but are clearly resolved and assigned by the ESI-FTICR-MS method.

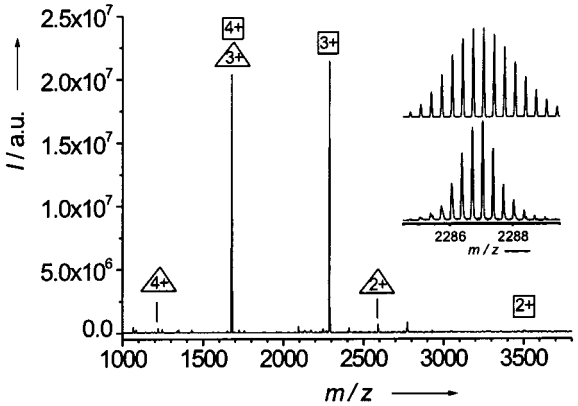

Figure 5. ESI-FTICR-MS (acetone solution) of triangle−square equilibrium **3d/4d**; the inset shows the calculated (top) and the experimental (bottom) isotopic distribution of the square species [**4d**-3OTf]$^{3+}$.

The results for complex **1b**−**2b** are in accordance to those for **1a**−**2b**, showing signals in the mass spectrum that originate from the triangle **3d** and the square **4d**. However, under the applied electrospray conditions (saturated acetone solution at room temperature) the two dominating intense signals in the spectrum arise exclusively from square **4d**, the [**4d**-3OTf]$^{3+}$ species at *m*/*z* 2287.038 and the [**4d**-4OTf]$^{4+}$ species at *m*/*z* 1677.795, whereas the signal intensities of the triangular species [**3d**-2OTf]$^{2+}$ (*m*/*z* 2591.271), [**3d**-3OTf]$^{3+}$ (*m*/*z* 1677.555), and [**3d**-4OTf]$^{4+}$ (*m*/*z* 1220.912) are only about 5−10% of those for the square signals (Figure 5). The inset in Figure 5 compares the measured isotopic distribution (bottom) of the 3-fold charged

(17) Assignment of the signal sets in the NMR spectra at elevated temperatures is tentatively on the basis of the observed inverse integral ratio of the two sets of signals in the *tert*-butylphenoxy systems **3c**−**d**/**4c**−**d** compared to the phenoxy systems **3a**−**b**/**4a**−**b**. The sterically demanding *tert*-butyl groups will favor the molecular square in the equilibrium, and therefore the dominating set of signals in **3c**−**d**/**4c**−**d** is assigned to the molecular squares. In the equilibria **3a**−**b**/**4a**−**b** the dominating set of signals is assigned to the molecular triangles, as is outlined in Figure 1 and Figure 2. This assignment is also in accordance with ESI-FTICR-MS signal intensities.

(18) (a) Amster, J. *J. Mass Spectrom.* **1996**, *31*, 1325−1337. (b) Marshall, A. G.; Hendrickson, C. L.; Jackson, G. S. *Mass Spectrom. Rev.* **1998**, *17*, 1−35.

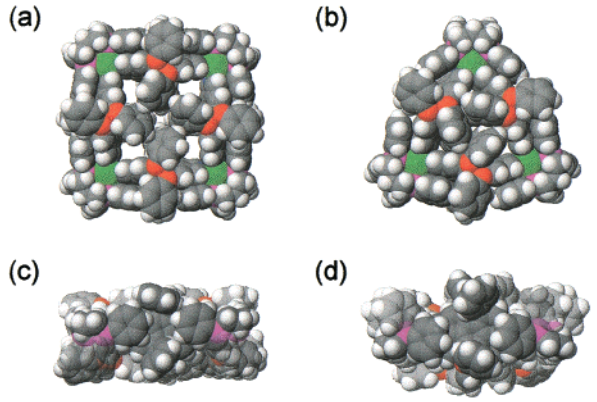

Figure 6. Side and top views of energy minimized structures of square **4a** (a,c) and triangle **3a** (b,d) obtained by molecular dynamics simulations and MM2 force field geometry optimizations. The steric crowding of the dppp-phenyl rings and the phenoxy groups of the diazadibenzoperylene ligands is most pronounced for square **4a** as visualized in (c).

square (resolution up to 65 000 fwhh) with the calculated one (top). A precise match between these two patterns could be observed for all signals.

The signal centered at *m*/*z* 1677 is again a superposition of trimeric and tetrameric as well as a singly charged species all of the same *m*/*z* ratio as found for the system **3b/4b**. An additional measurement at ultrahigh resolution revealed the presence of these three species at the given *m*/*z* ratio. It is of course not possible to quantify the equilibria by ESI-MS, but it is noteworthy that the ratios are in fairly good agreement with the situation in solution assigned by NMR spectroscopy.

Further evidence for the presence of dynamic triangle−square equilibria was obtained from an ESI-FTICR-MS exchange experiment. The platinum complexes **3b/4b** and **3d/4d** were mixed in acetone in a 1:1 stoichiometry. In the resulting ESI-FTICR mass spectra mixed species of triangles and squares containing both diaza ligands **1a** and **1b** could be unambiguously identified by their masses and charge states.[19]

Molecular Modeling. To gain insight into the dynamic behavior observed in the NMR spectra of the triangular and square species, and to find arguments why the (expected) molecular squares equilibrate with triangles, we applied molecular dynamics simulations that afforded plausible energy minimized structures of both triangles and squares.[20] The obtained energetically minimized structures are depicted in Figure 6.

It is obvious that there is considerable steric strain in both cyclic assemblies rendering these metallacycles thermodynamically less stable than other squares[4] reported by us and others (for stability studies, see below). The diazadibenzoperylene ligands have a highly twisted and nonflexible aromatic backbone[14] which is further rigidified when incorporated into the macrocycles. Herein $\pi-\pi$ contacts are given between two phenyl groups of the dppp ligand and the π-surface of the diazadibenzoperylene ligands which typically stabilize tetrameric assemblies.[4,13] However, as shown in the side views of both assemblies, it is exactly this structural feature which interferes considerably with the spatial demand of the phenoxy substituents of our diazadibenzoperylene ligands, especially within the square scaffold (Figure 6a,c). Significantly more space is available at the outer side of the triangle, thus making the latter energetically more favorable despite the less ideal geometry at the metal centers (Figure 6d).[21] Another feature that becomes important when we consider **3c/4c** and **3d/4d** is the smaller inner volume of the triangle which should lead to a sterically very critical encounter of the three *tert*-butylphenoxy groups at the top and bottom inner sides. Therefore, the reverse preference for the triangle/square species for the two phenoxy substituents observed by NMR and ESI-FTICR-MS is well-explained by these molecular modeling studies.

To explain the dynamic behavior observed in NMR spectroscopy we account the following features, which we also believe to be of importance in governing the equilibria. (i) The diazadibenzoperylene backbone is twisted as revealed by an X-ray crystal structure of a closely related ligand with a twisting angle of about 25° in the solid state.[14] In solution fast flipping averages this twisting, and the high flexibility of the phenoxy substituents afford the good solubility properties of these molecules. (ii) The somewhat bulky phosphane (dppp) ligands wrap around the coordinating pyridine units of the diazadibenzoperylenes with their phenyl rings such as a tweezer that results in favorable $\pi-\pi$ contacts. This interaction has been observed in X-ray crystal structures,[13] and it has been reported that in solution this interaction leads to broad NMR resonances of both pyridine and dppp protons that show a distinct temperature dependence.[4f,10g,13] (iii) There is an inner and outer region of the macrocycles and one should expect splitting of the ^{1}H NMR resonances of the phenoxy and perylene core protons at low temperatures when the structure is rigid and rotation is slow on the NMR time scale caused by steric hindrance and other intermolecular interactions. High temperatures lead to a high conformational flexibility (flipping of the perylene backbone, fast dppp dynamics and rotations of the perylene ligands) with fast processes on the NMR time scale pretending a high symmetry of the two species, resulting in simple sets of NMR resonances. At room-temperature coalescence is reached, and at lower temperatures there is a loss of conformational flexibility, and rotations and other dynamic processes become slow on the NMR time scale and therefore lead to abundant sharp resonances, owing to the reduction of symmetry.

Optical Properties. The metallacycles **3a**−**d**/**4a**−**d** exhibit strong absorption with maxima at 512 ± 2 nm and 480 ± 2 nm (CH_2Cl_2) which originate from the diazadibenzoperylene chromophore. From Figure 7a we see a bathochromic shift of 15 ± 1 nm for the S_0-S_1 transition of this chromophore in the UV/vis absorption spectra upon metal coordination. In addition, there are strong changes in the intensities of the spectral fine structure of the phenoxy-substituted systems **3a/4a** and **3b/4b** compared to the diazadibenzoperylene ligand **1a**. For the *tert*-butylphenoxy-substituted systems **3c/4c** and **3d/4d** the intensity changes in the spectral fine structure are less pronounced (Figure 7a).[22]

(19) Selected experimental *m*/*z* values of mixed intact triangle and square species: [(**1a1b$_2$2b$_3$**)-3OTf]$^{3+}$ *m*/*z* 1602.813; [(**1a$_2$1b2b$_3$**)-2OTf]$^{2+}$ *m*/*z* 2366.561; [(**1a$_3$1b2b$_4$**)-3OTf]$^{3+}$ *m*/*z* 2062.155.

(20) CAChe 3.2, Oxford Molecular **1999**. MD-MM2 simulation at 300 K using the CAChe 3.2 program.

(21) Entropy should also favor the formation of triangles as they assemble from fewer components with respect to squares.

(22) It is not yet clear to us what exactly causes these spectral changes. A possible reason for the changes in the spectral fine structures might be rigidification of the diazadibenzoperylene chromophores in the assemblies as suggested by molecular modeling and the observed NMR dynamics. Because the chromophores are more tightly assembled in the triangles than in the squares, stronger changes in the intensity of vibronic transitions are reasonable for the phenoxy-substituted systems **3a/4a** and **3b/4b** because of a higher triangle-to-square ratio compared to the *tert*-butylphenoxy-substituted systems **3c/4c** and **3d/4d**. Of course, other effects may also be involved, such as excitonic coupling between the chromophores. For the squares, excitonic coupling is expected to be negligible because of the orthogonal arrangement of adjacent chromophores and the large distances of ca. 1.5 nm between opposite chromophores. In the triangles the angle between adjacent chromophores is significantly smaller than 90°, and the

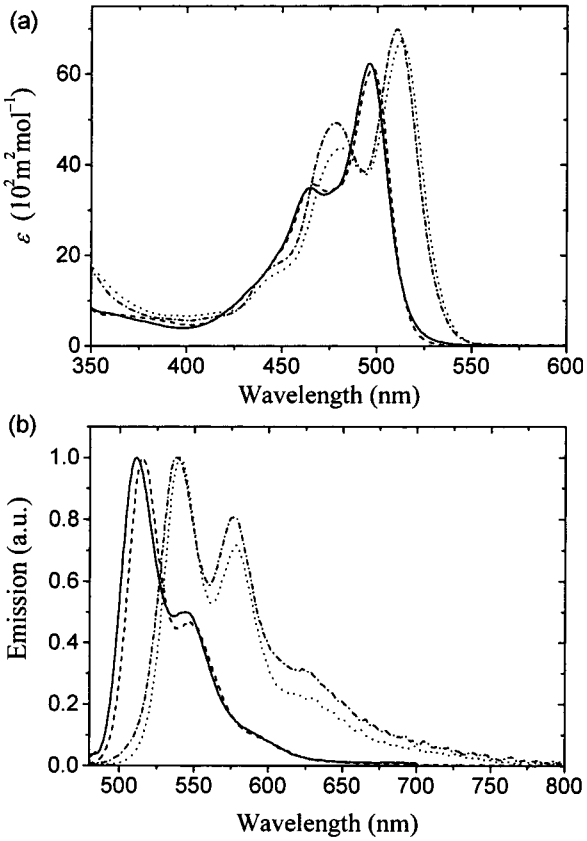

Figure 7. (a) UV/vis absorption spectra of **1a** (—), **1b** (- - -), **3b/4b** (-·-·-·), and **3d/4d** (···). (b) Fluorescence spectra of **1a** (—), **1b** (- - -), **3b/4b** (-·-·-·) and **3d/4d** (···). All spectra were recorded in CH_2Cl_2 (ϵ values were calculated with respect to the concentrations of the chromophores **1a,b**).

In contrast to the previously reported perylene bisimide-based molecular squares which exhibited fluorescence quantum yields around 90%,[4f−g] here the intense diazadibenzoperylene fluorescence ($\Phi_F = 0.75$) is strongly quenched upon metal coordination. Weak emission of the complexes occurs with maxima at 540 ± 1 nm and 576 ± 2 nm and a quantum yield which is by a factor of 10^5 to 10^6 lower than for **1a,b** (Figure 7b).

To obtain further information on the stability of the metallacycles we followed the process of coordination by UV/vis and fluorescence dilution studies (Figure 8). Upon diluting a 10^{-4} M concentrated solution of **3a/4a** (CH_2Cl_2), the maximum absorption band and the high-energy shoulder are gradually shifted to shorter wavelengths, eventually resulting in the absorption spectrum of the free ligand **1a**. At the same time the intensity of the high-energy shoulder at $\lambda = 478$ nm decreases. Figure 8 shows a logarithmic plot of the extinction coefficient at this indicative wavelength versus concentration, resulting in a sigmoid curve that exhibits a narrow concentration range between 10^{-5} and 10^{-6} M, where complex formation−dissociation processes take place. The same dilution study monitored by fluorescence spectroscopy reveals a similar signature if the normalized integrated emission (that is corrected for the optical density at the excitation wavelength) is plotted versus concentration. For both graphs the points of inflection are located at the same concentrations of 3×10^{-6} M, indicating that the same species in the equilibria are detected by both spectroscopic techniques. Finally, the same experiment was performed with the platinum complex **3b/4b** (CH_2Cl_2), and similar curves were obtained (Figure 8). However, the concentration range, where complex dissociation occurs, is at lower concentrations with a point of inflection at 1×10^{-6} M, providing evidence for the higher stability of platinum coordination compared to that of palladium coordination.

chromophore to chromophore center distances are considerably smaller; hence, spectral changes due to excitonic coupling might be of importance.

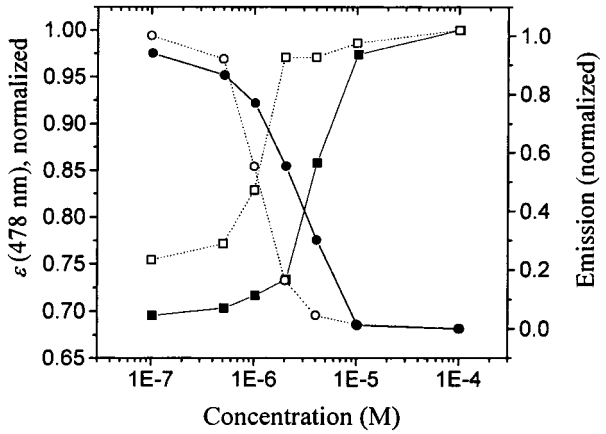

Figure 8. Dilution study monitored by the concentration dependence of the UV/vis absorption coefficient at 478 nm (**3a/4a** (■—) and **3b/4b** (□- - -)) and normalized integrated emission corrected for the optical density at the excitation wavelength (**3a/4a** (●—) and **3b/4b** (○- - -)).

Conclusions

Transition metal-directed self-assembly of substituted diazadibenzoperylene bridging ligands **1a,b** with Pd(II)− and Pt(II)−phosphane corners **2a,b** resulted in unexpected equilibria between molecular triangles **3a**−**d** and molecular squares **4a**−**d**. Owing to complex dynamics on the NMR time scale, identification and characterization of the species could only be accomplished by a combination of variable-temperature ^1H and $^{31}P\{^1H\}$ NMR spectroscopy and ESI-FTICR mass spectrometry. By employing different metal ions, Pd(II) and Pt(II), and two diazadibenzoperylene ligands that differ only in their phenoxy substituents, energetic as well as steric effects that govern the triangle−square equilibria could be investigated. Molecular modeling helped to draw a reasonable picture of the steric situation of the triangular and square structures. The absorption properties of the diazadibenzoperylene chromophores are affected considerably by metal coordination, and fluorescence is strongly quenched. The higher stability of the platinum complexes with respect to the palladium complexes could be proven by dilution studies of the complexes which revealed dissociation processes in the micro- to nanomolar range.

Experimental Section

Materials and Methods. Solvents and reagents were purchased from Merck unless otherwise stated and purified and dried according to standard procedures.[23] $[Pd(dppp)][(OTf)_2]\cdot 2H_2O$ (dppp = 1,3-bis(diphenylphosphino)propane; OTf = trifluoromethanesulfonate) and $[Pt(dppp)][(OTf)_2]\cdot 2H_2O$[13] were synthesized according to the literature. UV/vis spectra were recorded on a Perkin-Elmer Lambda 40P spectrometer. All ϵ values are given with respect to the concentration of the diazadibenzoperylene chromophores. Corrected fluorescence spectra were recorded on a Perkin-Elmer LS 50B fluorometer. ^1H NMR spectra were recorded on a Bruker AMX 500 spectrometer at 500 MHz, and chemical shifts are reported relative to the signal of residual protonated nitromethane δ 4.33 ppm. The $^{31}P\{^1H\}$ NMR spectra were recorded at 202 MHz, and chemical shifts are reported relative to

(23) Perrin, D. D.; Armarego, W. L. F. *Purification of Laboratory Chemicals*, 2nd ed;, Pergamon Press: Oxford, 1980.

external 85% aqueous H_3PO_4 δ 0.0 ppm. ESI-FTICR-MS measurements were carried out with a passively shielded 4.7 T APEXII-ESI/MALDI-FT-ICR-mass spectrometer from Bruker Daltonik (Bremen, Germany). Saturated solutions of the complexes in acetone were prepared. For mass calculation, data acquisition, processing, apodization, and deconvolution the mass spectrometry software XMASS version 5.0.7 (Bruker Daltonik) was used. The number of data points was 512 K for acquisition and 1 M for processing within a mass range of 600−4000 Da. To increase the signal-to-noise-ratio 100 scans were accumulated. For the external four-point-calibration an ES Tuning Mix from Hewlett-Packard (Waldbronn, Germany) was used.

The synthesis of **1a** has been recently described in detail.[14] The same synthetic protocol was used for the synthesis of the *tert*-butyl-substituted analogue **1b** (refer to Supporting Information).

Metallacycles 3a/4a. 5,6,12,13-Tetraphenoxy-2,9-diazadibenzo-[*cd*,*lm*]perylene **1a** (50.0 mg, 0.072 mmol) and [Pd(dppp)][$(OTf)_2$]·$2H_2O$ **2a** (61.3 mg, 0.072 mmol) were stirred at room temperature under argon in CH_2Cl_2 (10 mL) for 24 h. After filtration the solution was concentrated to ca. 1 mL, and an orange solid was precipitated upon addition of diethyl ether. The product was separated by centrifugation, washed twice with diethyl ether, and dried in vacuo to yield 86 mg (78%). Mp 304−306 °C dec. ^{1}H NMR (500 MHz, CD_3NO_2, 353 K) **3a:** δ 9.11 (s, 12H, H_α), 7.73 (m, 24H, H_{dppp}), 7.41 (t, 24H, ^3J = 7.5 Hz, H_{PhO}), 7.37 (s, 12H), 7.22 (m, 12H, H_{PhO}), 7.16 (m, 24H, H_{dppp}), 7.09 (m, 12H, H_{dppp}), 6.92 (d, 24H, ^3J = 7.5 Hz, H_{PhO}), 3.26 (s(br), 12H, H_{dppp}), 2.43 (s(br), 6H, H_{dppp}); **4a:** δ 9.38 (s, 16H, H_α), 7.62 (m, 32H, H_{dppp}), 7.38 (s, 16H), 7.34 (t, 32H, H_{PhO}), 7.29 (m, 16H, H_{dppp}), 7.27 (m, 16H, H_{PhO}), 7.06 (m, 32H, H_{dppp}), 6.94 (d, 32H, H_{PhO}), 3.21 (s(br), 16H, H_{dppp}), 2.43 (s(br), 8H, H_{dppp}). ^{31}P{^{1}H} NMR (202 MHz, CD_3NO_2, 353 K, 85% H_3PO_4) **3a:** δ 11.31 (s); **4a:** δ 10.42 (s). UV−vis (CH_2Cl_2, 293 K) λ_{max} (ϵ) [nm (mol^{-1} dm^3 cm^{-1})] 510 (68 100), 478 (49 100), 333 (30 900), 293 (83 200); Fluorescence (CH_2Cl_2, 293 K) 541, 575 nm. Anal. Calcd for ($C_{77}H_{54}N_2O_{10}F_6P_2PdS_2$·$H_2O$)$_n$ (n·1531.8) C, 60.38; H, 3.68; N, 1.83; S 4.19. Found: C, 60.29; H, 3.89; N, 1.68; S, 4.00.

Metallacycles 3b/4b. 5,6,12,13-Tetraphenoxy-2,9-diazadibenzo-[*cd*,*lm*]perylene **1a** (50.0 mg, 0.072 mmol) and [Pt(dppp)][$(OTf)_2$]·$2H_2O$ **2b** (67.6 mg, 0.072 mmol) were reacted and worked up as described for **3a, 4a** to yield 75 mg (64%) of an orange solid. Mp >310 °C. ^{1}H NMR (500 MHz, CD_3NO_2, 353 K) **3b:** δ 9.09 (s, 12H, H_α), 7.73 (m, 24H, H_{dppp}), 7.43 (t, 24H, H_{PhO}), 7.40 (s, 12H), 7.32−7.05 (m, obscured and overlap with signals of **4b**, 12H + 24H + 12H, H_{PhO} + H_{dppp} + H_{dppp}), 6.93 (d, 24H, H_{PhO}), 3.32 (s(br), 12H, H_{dppp}), 2.40 (s(br), 6H, H_{dppp}); **4b:** δ 9.35 (s, 16H, H_α), 7.63 (m, 32H, H_{dppp}), 7.37 (t, 32H, H_{PhO}), 7.35 (s, 16H), 7.32−7.05 (m, obscured and overlap with signals of **3b**, 16H + 32H + 16H, H_{PhO} + H_{dppp} + H_{dppp}), 6.95 (d, 32H, H_{PhO}), 3.27 (s(br), 16H, H_{dppp}), 2.40 (s(br), 8H, H_{dppp}). ^{31}P{^{1}H} NMR (202 MHz, CD_3NO_2, 353 K, 85% H_3PO_4) **3b:** δ −11.14 (s); **4b:** δ −11.65 (s). UV−vis (CH_2Cl_2, 293 K) λ_{max} (ϵ) [nm (mol^{-1} dm^3 cm^{-1})] 510 (69 900), 478 (49 300), 335 (25 200), 324 (24 900), 294 (79 900). Fluorescence (CH_2Cl_2, 293 K) 539, 576 nm. Anal. Calcd for ($C_{77}H_{54}N_2O_{10}F_6P_2PtS_2$·$2H_2O$)$_n$ (n·1638.5) C, 56.45; H, 3.57; N, 1.71; S, 3.91. Found C, 56.47; H, 3.53; N, 1.65; S, 3.84.

Metallacycles 3c/4c. 5,6,12,13-Tetra(4-*tert*-butylphenoxy)-2,9-diazadibenzo-[*cd*,*lm*]perylene **1b** (24.4 mg, 0.027 mmol) and [Pd(dppp)][$(OTf)_2$]·$2H_2O$ **2a** (22.6 mg, 0.027 mmol) were reacted and worked up as described for **3a, 4a** to yield 33 mg (70%) of an orange solid. Mp >310 °C. ^{1}H NMR (500 MHz, CD_3NO_2, 353 K) **3c:** δ 9.15 (s, 12H, H_α), 7.75 (m, 24H, H_{dppp}), 7.51 (d, ^3J = 8.4 Hz, 24H, H_{PhO}), (7.34 (s (br), 36H, H_{dppp})), 6.92 (d, ^3J = 8.4 Hz, 24H, H_{PhO}), 3.27 (s(br), 12H, H_{dppp}), 2.39 (s(br), 6H, H_{dppp}), 1.49 (s, 108H, H_{tBu}); **4c:** δ 9.43 (s, 16H, H_α), 7.63 (m, 32H, H_{dppp}), 7.38 (d, ^3J = 8.4 Hz, 32H, H_{PhO}), (7.13 (s, 4H, 16H, $H_{perylene}$)), 7.04 (m, 48H, H_{dppp}), 6.86 (d, ^3J = 8.4 Hz, 32H, H_{PhO}), 3.22 (s(br), 16H, H_{dppp}), 2.39 (s(br), 8H, H_{dppp}), 1.37 (s, 36H, H_{tBu}). ^{31}P{^{1}H} NMR (202 MHz, CD_3NO_2, 353 K, 85% H_3PO_4) **3c:** δ 11.19 (s); **4c:** δ 10.16 (s). UV−vis (CH_2Cl_2, 293 K) λ_{max} (ϵ) [nm (mol^{-1} dm^3 cm^{-1})] 513 (67 300), 481 (43 800), 336 (23 400), 294 (70 200), 286 (61 500). Fluorescence (CH_2Cl_2, 293 K) 541, 575 nm. Anal. Calcd for ($C_{93}H_{86}N_2O_{10}F_6P_2PdS_2$·$H_2O$)$_n$ (n·1756.2) C, 63.61; H, 5.05; N, 1.60; S, 3.65. Found C, 63.71; H, 5.11; N, 1.56; S, 3.37.

Metallacycles 3d/4d. 5,6,12,13-Tetra(4-*tert*-butylphenoxy)-2,9-diazadibenzo-[*cd*,*lm*]perylene **1b** (36.9 mg, 0.04 mmol) and [Pt(dppp)][$(OTf)_2$]·$2H_2O$ **2b** (37.7 mg, 0.04 mmol) were reacted and worked up as described for **3a, 4a** to yield 41 mg (55%) of an orange solid. Mp >310 °C. ^{1}H NMR (500 MHz, CD_3NO_2, 353 K) **3d:** δ 9.11 (s, 12H, H_α), 7.76 (m, 24H, H_{dppp}), 7.52 (d, ^3J = 8.4 Hz, 24H, H_{PhO}), (7.19 (m, 36H, H_{dppp})), (7.16 (s, 12H, $H_{perylene}$)), 6.92 (d, ^3J = 8.4 Hz, 24H, H_{PhO}), 3.33 (s(br), 12H, H_{dppp}), 2.39 (s(br), 6H, H_{dppp}), 1.50 (s, 108H, H_{tBu}); **4d:** δ 9.40 (s, 16H, H_α), 7.64 (m, 32H, H_{dppp}), 7.39 (d, ^3J = 8.4 Hz, 32H, H_{PhO}), 7.36 (s, 4H, 16H, $H_{perylene}$), 7.06 (m, 48H, H_{dppp}), 6.87 (d, ^3J = 8.4 Hz, 32H, H_{PhO}), 3.28 (s(br), 16H, H_{dppp}), 2.39 (s(br), 8H, H_{dppp}), 1.38 (s, 36H, H_{tBu}). ^{31}P{^{1}H} NMR (202 MHz, CD_3NO_2, 353 K, 85% H_3PO_4) **3d:** δ −11.31 (s); **4d:** δ −12.07 (s). UV−vis (CH_2Cl_2, 293 K) λ_{max} (ϵ) [nm (mol^{-1} dm^3 cm^{-1})] 513 (68 500), 481 (45 700), 334 (29 300), 294 (78 400). Fluorescence (CH_2Cl_2, K) 540, 578 nm. Anal. Calcd for ($C_{93}H_{86}N_2O_{10}F_6P_2PtS_2$·$2H_2O$)$_n$ (n·1862.9) C, 59.96; H, 4.87; N, 1.50; S, 3.44. Found C, 60.25; H, 4.88; N, 1.50; S, 3.50.

Acknowledgment. F. W. is indebted to the Fonds der Chemischen Industrie and BMBF for a Liebig Grant and to DFG for a Habilitation Grant. We gratefully acknowledge the Ulmer Universitätsgesellschaft for a startup grant for this project, BASF AG and Degussa-Hüls AG for the donation of chemicals.

Supporting Information Available: Preparation and physical properties of **1b** (PDF). This material is available free of charge via the Internet at http://pubs.acs.org.

JA004360Y